# Dirac Phenomenological Analyses for the High-lying Excited States of the Gamma Vibrational Band at $^{58}$Ni(p, p')

## Sugie Shim*

*Physics Department, Kongju National University, Gonjusi, Republic of Korea*

**Abstract:** *Relativistic Dirac phenomenological analysis based on the Dirac equation is performed for the inelastic scatterings of intermediate energy proton from the $^{58}$Ni nucleus. Dirac coupled channel equations are solved phenomenologically using an optical potential model. A vibrational collective model is used to describe the high-lying excited states of the gamma vibrational band. The results obtained by using the Dirac phenomenological coupled channel calculations are observed to agree reasonably well with the inelastic scattering experimental data, showing a little better agreements with the data than those obtained in the nonrelativistic calculations. The channel coupling effect for the high-lying excited states those belong to the gamma vibrational band at the axially symmetric deformed nucleus is also investigated.*

**Keywords:** *Dirac phenomenology, Coupled channel analyses, Proton inelastic scattering, Collective model, Optical potential model*

## 1. INTRODUCTION

Relativistic Dirac phenomenological approaches based on the Dirac equation have shown remarkably successful results in treating nuclear reactions compared to the conventional nonrelativistic approaches based on the Schroedinger equation [1-6]. Dirac phenomenological coupled channel analyses of proton inelastic scatterings from the spherically symmetric nuclei and several deformed nuclei are performed successfully [7-11]. However, it is still necessary to expand Dirac phenomenological analysis to the intermediate energy scatterings from various nuclei in order to have systematic analyses of relativistic calculations.

In this work we perform Dirac phenomenological coupled channel analyses for the 800 MeV proton inelastic scattering from $^{58}$Ni nucleus, for which the relativistic Dirac analysis has not been reported so far. The optical potential model [1, 4] is used, employing S-V model [4, 7] where only scalar and time-like vector optical potentials are considered. A first order

vibrational collective model [8] is used in order to obtain the transition optical potentials to describe the collective motion of the excited deformed nucleus considering the high-lying excited states of the gamma vibrational band [11]. The third $2^+$ and the second $4^+$ states are assumed to be members of the $K^\pi=2^+$ gamma vibrational band. The multistep process is included in the calculation by considering the channel coupling between two excited states [12, 13]. Dirac optical potential and the deformation parameters are phenomenologically determined by fitting the elastic and inelastic scattering experimental data using a computer program called ECIS [14]. The obtained deformation parameters and optical potential parameters are analyzed and compared with those obtained in the nonrelativistic calculations.

## 2. THEORY AND RESULTS

Relativistic Dirac phenomenological analysis of 800 MeV proton scattering from the $^{58}$Ni nucleus is performed using an optical potential model and the first order collective model in the Dirac coupled channel formalism. The Dirac equation for the nucleon-nucleus elastic scattering for the spin 0 nucleus [6] is given as

$$[\alpha \cdot p + \beta(m + U_S) - (E - U_V^0 - V_C) + i\alpha \cdot \hat{r}\beta U_T]\Psi(r) = 0,$$

where $U_S$ is a scalar potential, $U_V^0$ a time-like vector potential, $U_T$ a tensor potential, and $V_C$ is the Coulomb potential. Only the scalar and the time-like vector potentials are used as direct potentials in the calculations. The tensor potentials are neglected in this calculation because they have been found to be always very small compared to the scalar or vector potentials [8], even though they are always present due to the interaction of the anomalous magnetic moment of the projectile with the charge distribution of the target. The scalar and time-like vector optical potentials are complex and it is assumed that these potentials have Fermi distribution as they are assumed to follow the distribution of nuclear density. Fermi model form factor of Woods-Saxon shape is used for the geometry

of the Dirac optical potentials. In the first order vibrational model of ECIS, the deformation of the radius of the optical potential is given using the Legendre polynomial expansion method;

$$R(\theta) = R_0(1 + \sum_{\lambda,\mu} \beta_\lambda Y^*_{\lambda\mu}(\theta,\varphi)),$$

with $R_0$ being the radius at equilibrium, $\beta_\lambda$ a deformation parameter and $\lambda$ the multipolarity. It is assumed that the shape of the deformed transition potentials follows the shape of the deformed nuclear densities and that the transition potentials can be obtained by assuming that they are proportional to the first-order derivatives of the diagonal potentials. However, it is true that pseudo-scalar and axial-vector potentials may also be present in the equation when we consider inelastic scattering, depending on the model assumed. In the collective model approach used in this work, we assume that we can obtain appropriate transition potentials by deforming the direct potentials that describe the elastic channel fairly well [7]. The transition potentials are obtained by setting to be proportional to the first derivatives of the diagonal potentials, as in Tassi model, assuming the shape of the deformed potentials follows the shape of deformed nuclear densities. We consider both couplings between the $0^+$ ground state and the excited states and also the couplings between two adjacent excited states. Hence the multistep channel coupling process is included in the calculation. Dirac coupled channel calculations are performed in which the phenomenological direct potential parameters are varied along with the deformation parameters. The Dirac coupled channel equations are solved numerically to reproduce the experimental observables using the computer code ECIS [14] which employs the sequential iteration method. The Schroedinger-like second order Dirac equation is obtained by considering the upper component of the Dirac wave function, and the effective complex central and spin-orbit optical potentials are obtained [7, 10] to be compared with the potentials obtained in the nonrelativistic Schroedinger calculations.

The experimental data for the differential cross sections are obtained from [15] for the 800 MeV proton elastic and inelastic scatterings from the $^{58}$Ni nucleus. The high-lying excited states of the gamma vibrational band ($K^\pi = 2^+$), $2_3^+$ (3.04 MeV) and $4_2^+$ (3.62 MeV) states are considered and assumed to be collective vibrational states in the calculation. At first, 12 parameters of the diagonal scalar and vector potentials in the Woods-Saxon shapes are phenomenologically determined to reproduce the experimental elastic scattering data. The Dirac equations are solved to obtain the best fitting

optical potential parameters to the experimental data by using the sequential iteration method. **Table 1** shows the 12 Woods-Saxon potential parameters obtained by fitting the elastic scattering data. Showing the same pattern as in the spherically symmetric nuclei [5, 9], the real scalar potentials and the imaginary vector potentials turn out to be large and negative, and that the imaginary scalar potentials and the real vector potentials turn out to be large and positive.

**Table 1:** *The optical potential parameters of Woods-Saxon shape obtained in the Dirac phenomenological calculations for the 800 MeV proton elastic scatterings from $^{58}$Ni nucleus.*

| Potential | Strength (MeV) | Radius (fm) | Diffusiveness (fm) |
|---|---|---|---|
| Scalar real | -328.3 | 3.795 | 0.764 |
| Scalar imaginary | 30.24 | 3.929 | 0.734 |
| Vector real | 205.2 | 3.821 | 0.691 |
| Vector imaginary | -84.97 | 3.978 | 0.654 |

As a next step, all of the optical potential-parameters and deformation parameters are searched by including the one excited state of the gamma vibrational band, the $2_3^+$ state or $4_2^+$ state, in addition to the ground state in the calculation, starting from the 12 parameters for the direct optical potentials obtained in the elastic scattering calculation. We searched for the two deformation parameters, $\beta_S$ and $\beta_V$, per each excited state by assuming the real and imaginary deformation parameters are the same [7-10]. Finally, we included all three states, $0^+$, $2_3^+$, and $4_2^+$ states, in the calculation in order to see the multistep channel coupling effect. The optical potential parameters obtained by fitting the elastic scattering data in the elastic scattering calculation are varied because the channel coupling of the excited states to the ground state should be included in the inelastic scattering calculation.
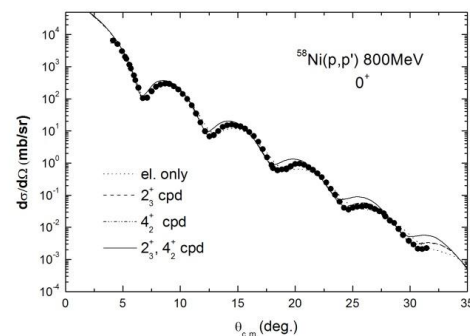


**Figure 1**: *Comparison of the results of Dirac coupled channel calculations with the ground state experimental data for 800 MeV proton inelastic scatterings from $^{58}$Ni nucleus.*
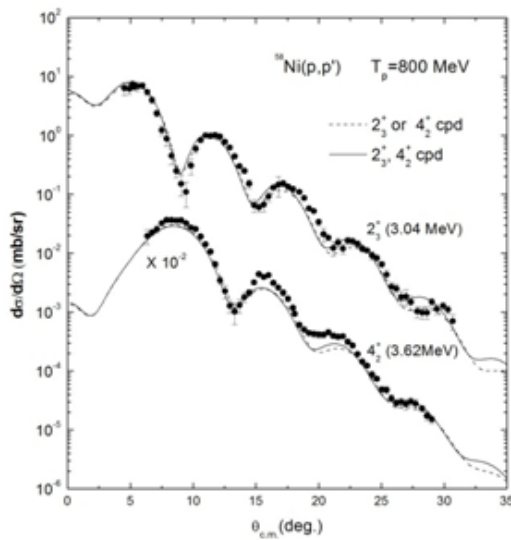
**Figure 2:** *Comparison of the results of Dirac coupled channel calculations with the $2_3^+$ and $4_2^+$ excited states of the gamma vibrational band experimental data for 800 MeV proton inelastic scatterings from $^{58}$Ni nucleus.*

The results of the Dirac coupled channel calculations for the ground state are shown in the **Figure 1** and it is shown that the relativistic Dirac coupled channel calculation using an optical potential model could describe the ground state for 800 MeV proton inelastic scatterings from the $^{58}$Ni nucleus reasonably well, except for the all three states coupled case. In figures, "cpd" means "coupled". The results of the coupled channel calculations for the $2_3^+$ and $4_2^+$ excited states in the gamma vibrational band are shown in the **Figure 2** and it is shown that relativistic Dirac coupled channel calculation using an optical potential model could describe the high-lying excited states of the gamma vibrational band for 800 MeV proton inelastic scatterings from the $^{58}$Ni nucleus reasonably well, showing better agreements with the experimental data than those obtained in the nonrelativistic calculations [15]. It is shown that the agreements with $2_3^+$ data are not improved significantly by adding $4_2^+$ state in the calculation, showing the channel coupling effect of the multistep is not important for the high-lying state excitations of the gamma vibrational band at the proton inelastic scattering from $^{58}$Ni nucleus. As shown in **Figure 2**, the results of the Dirac coupled channel calculations for the $4_2^+$ excited state in the gamma virational band could not describe the experimental data very well, missing the second maximum and minimum points of the data, even though the results of the relativistic calculation could reproduce the data slightly better than those obtained in the nonrelativistic calculations [15].

**Table 2:** *Comparison of the deformation parameters of the high-lying excited states of the gamma vibrational band obtained in the relativistic Dirac coupled channel calculations with those obtained in the nonrelativistic calculations [15. 16] for the 800 MeV proton inelastic scatterings from $^{58}$Ni nucleus.*

|  | $\beta_S$ | $\beta_V$ | $\beta_{NR}$ |
|---|---|---|---|
| $2_3^+$ cpd. | 0.049 | 0.061 | 0.070[15], 0.067[16] |
| $4_2^+$ cpd. | 0.055 | 0.068 | 0.093[15], 0.080[16] |
| $2_3^+$, | 0.042 | 0.053 |  |
| $4_2^+$ cpd. | 0.043 | 0.056 |  |

In **Table 2**, we show the deformation parameters for the $2_3^+$ and $4_2^+$ excited states of the $^{58}$Ni nucleus obtained in the relativistic Dirac coupled channel calculations and compare them with those obtained in the nonrelativistic calculations [15. 16]. It is observed that the deformation parameters obtained in the Dirac phenomenological coupled channel calculation for the $2_3^+$ and $4_2^+$ state excitations of the $^{58}$Ni nucleus show reasonably good agreement with those obtained in the nonrelativistic calculations, using the same Woods-Saxon shape for the geometry of the potentials, even thogh they used distorted wave Born approximation in Ref. 15 and they considered low energy proton scattering in Ref. 16.
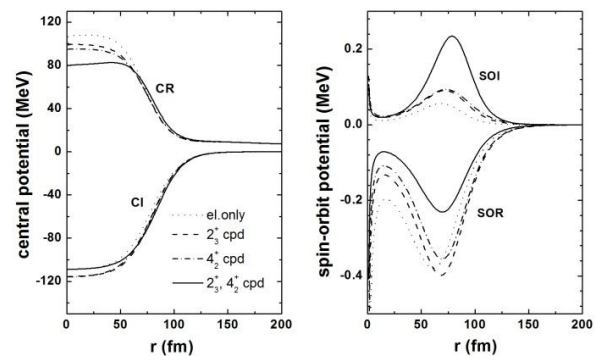


**Figure 3:** *The effective central and spin-orbit potentials of $^{58}$Ni nucleus. CR and CI represent central real and imaginary potentials, and SOR and SOI represent spin-orbit real and imaginary optical potentials, respectively.*

In **Figure 3**, we show the effective central and spin-orbit potentials of the $^{58}$Ni nucleus. We show the effective potentials for the cases of elastic calculation (dotted line), where the ground and $2_3^+$ states are coupled (dashed line), where the ground and $4_2^+$ states are coupled (dash-dotted line), and where all three states are coupled (solid line). Surface-peaked phenomena are not clearly observed for the effective central potentials for the scattering from $^{58}$Ni nucleus.

The surface-peaked phenomena are clearly shown at the effective spin-orbit potentials, and the effective spin-orbit potential strengths turned out to be about the same order with those obtained from nonrelativistic calculations [15], even though the sign is the opposite for the real spin-orbit potential. It should be noted that one of the merits of the relativistic approach based on the Dirac equation instead of using the nonrelativistic approach based on the Schroedinger equation is that the spin-orbit potential appears naturally in the Dirac approach when the Dirac equation is reduced to a Schroedinger-like second-order differential equation, while the spin-orbit potential should be inserted by hand in the conventional nonrelativistic Schroedinger approach.

## 3. CONCLUSIONS

Relativistic Dirac coupled channel analyses are performed for the 800 MeV proton inelastic scatterings from $^{58}$Ni nucleus using an optical potential model. The optical potential parameters are dertermined phenomenologically using the scalar-vector potential model. It is shown that the theoretical results of the relativistic Dirac calculations reproduce the experimental data reasonably well, showing a little better agreements with the experimental data than those obtained in the nonrelativistic calculations. The channel coupling effect of the multistep process turns out to be not significant for the high-lying state excitations of the gamma vibrational band at the proton inelastic scattering from $^{58}$Ni nucleus. By reducing Dirac equations to the Schroedinger-like second-order differential equations, the effective central and spin-orbit potentials are obtained and the surface-peaked phenomena are not clearly observed at the effective central potentials for the proton scattering from $^{58}$Ni nucleus. The first-order vibrational collective models are used to describe the high-lying excited states of the gamma vibrational bands in the $^{58}$Ni nucleus, and the obtained deformation parameters are found to agree reasonably well with those of the nonrelativistic calculations.

## ACKNOWLEDGEMENT

## REFERENCES

[1] L. G. Arnold, B. C. Clark, R. L. Mercer, and P. Swandt, "Dirac optical model analysis of p – $^{40}$Ca elastic scattering at 180 MeV and the wine-bottle-bottom shape", *Phys. Rev. C*, Vol. 23, pp. 1949-1959, 1981

[2] C. J. Horowitz and B. D. Serot, "Self-consistent hartree description of finite nuclei in a relativistic quantum field theory", Nucl. Phys. A vol. 368, pp. 503-528, 1981.

[3] M. R. Anastasio, L. S. Celenza, W. S. Pong, and C. M. Shakin, "Relativistic nuclear structure physics", Physics Reports, vol. 100, pp. 327-401, 1983.

[4] J. A. McNeil, J. Shepard, and S. J. Wallace, "Impulse-approximation Dirac optical potential", Phys. Rev. Lett, vol. 50, pp. 1439-1442, 1983.

[5] L. S. Celenza and C. M. Shakin, "Relativistic nuclear physics", World Scientific, New-York, 1986.

[6] R. J. Furnstahl, C. E. Price, and G. E. Walker, "Systematics of light deformed nuclei in relativistic mean-field models", Phys. Rev. C vol. 36, pp. 2590-2600, 1987.

[7] S. Shim, "Relativistic analyses of nucleon-nucleus inelastic scatterings", Ph.D. Thesis, The Ohio State University, U. S. A., 1989.

[8] S. Shim, B. C. Clark, E. D. Cooper, S. Hama, R. L. Mercer, L. Ray, J. Raynal, and H. S. Sherif, "Comparison of relativistic and nonrelativistic approaches to the collective model treatment of $p+^{40}$Ca inelastic scattering", Phys. Rev. C, vol. 42, pp. 1592-1597, 1990.

[9] S. Shim, M. W. Kim, B. C. Clark, and L. Kurth Kerr, "Dirac coupled channel analyses of 800 MeV proton inelastic scattering from $^{24}$Mg", *Phys. Rev. C*, Vol. 59, No. 1, pp. 317-322, 1999.

[10] S. Shim and M. W. Kim, "Systematic Dirac Analyses of Proton Inelastic Scatterings from Axially Symmetric Deformed Nuclei", *Int. Jou. of Mod. Phys. E*, Vol. 21, No. 12, pp. 1250098.1-1250098.10, 2012.

[11] S. Shim, "Relativistic Dirac analyses of polarized proton scatterings to the $2^+$ gamma vibrational band in $^{24}$Mg and $^{26}$Mg", Can. J. phys., vol 95, pp 317-321, 2017.

[12] M. L. Barlett, J. A. McGill, L. Ray, M. M. Barlett, G. W. Hoffmann, N. M. Hintz, G. S. Kyle, M. A. Franey, and G. Blanpied, "Proton scattering from $^{154}$Sm and $^{176}$Yb at 0.8 GeV", Phys. Rev. C, vol. 22, pp. 1168-1179, 1980.

[13] S. Shim, and M. W. Kim, "Relativistic analysis of proton inelastic scattering from an axially symmetric deformed nucleus", New Physics, vol. 40, pp. 545-553, 2000.

[14] J. Raynal, "Computing as a language of physics", ICTP International Seminar Course, 281, IAEA, Italy, 1972; J. Raynal, Notes on ECIS94, Note CEA-N-2772, 1994.

[15] G. S. Kyle, N. M. Hintz, M. S. Oothoudt, M. Kaletka, P. M. Lang *et al*, "Elastic and inelastic scattering of 800 MeV protons by $^{58}$Ni", Phys. Lett., Vol. 91B, pp. 353-357, 1980.

[16] K. Thompson, Thesis, Michigan State Univ., U.S.A., 1969.